Energy 123 (2017) 173–188

Contents lists available at ScienceDirect

Energy

journal homepage: www.elsevier.com/locate/energy

Integrated modelling of variable renewable energy-based power supply in Europe

Hans Christian Gils*, Yvonne Scholz, Thomas Pregger, Diego Luca de Tena [1], Dominik Heide [2]

DLR - German Aerospace Center, Institute of Engineering Thermodynamics, Pfaffenwaldring 38-40, 70569 Stuttgart, Germany

ARTICLE INFO

Article history:
Received 1 March 2016
Received in revised form
17 January 2017
Accepted 22 January 2017
Available online 30 January 2017

Keywords:
Energy system modelling
Variable renewable energy
Power supply
Storage
Europe

ABSTRACT

Variable renewable energy (VRE) resources increasingly add fluctuations to power systems. The required types and capacities of balancing measures, amounts of curtailment, and costs associated with system integration need to be assessed for advising policy makers and economic actors. Previous studies mostly exclude storage from model-endogenous capacity expansion and omit concentrated solar power (CSP) completely. In this study, we stress the need for grid and backup capacity by investigating an integrated market in Europe, allowing for additional short-term as well as long-term storage and considering CSP as a dispatchable backup option. The Renewable Energy Mix (REMix) energy system model is introduced and applied to assess the capacity expansion and hourly dispatch at various levels of photovoltaic and wind power penetration. The model results demonstrate combinations of spatial and temporal balancing measures that enable net photovoltaic and wind supply shares of 60% and 70% of the annual demand, respectively. The usage of storage and grid can keep curtailments below 20% of the demand for theoretical VRE shares of up to 100%. Furthermore, we determine that the VRE supply structure has a strong impact on the least-cost allocation of power plants across Europe but only a limited effect on supply costs.

List of symbols

1. Introduction and state of research

Variable renewable energy (VRE) resources are expected to largely contribute to the future European power supply owing to their low CO_2 emissions, decreasing cost, widespread availability, and high potential compared with stored or storable resources. The substantial fluctuations of power generation that accompany high VRE shares require balancing measures such as transmission, storage and backup power generation, demand-side management, energy sector coupling, and curtailment. The central questions that arise for policy makers and electric utility companies planning the development of supply systems can be formulated as follows: What are the balancing requirements at various shares of VRE penetration and which technologies are suitable for guaranteeing a reliable supply at low costs?

Research questions challenging the operation and capacity expansion of power supply technologies are typically assessed by the application of energy system models. Such models have been developed with different scopes and methodologies and have been in use for decades. With improved computing power, these models have increased in both the level of detail and size. A general introduction to the aims and methods of energy system models has been reported by Ref. [1]. Detailed introductions and comparisons of manifold energy tools are also available [2,3].

Systematic investigations of the required integration measures at different VRE shares and mixes of solar and wind energy in Europe have been conducted recently. Physical approaches focusing on minimum backup capacity, backup energy, or curtailed energy amounts have been applied in previous research [4–8]. In these studies, VRE mixes between 30% and 50% solar photovoltaic and 50%–70% wind power generation are reported to be easiest to integrate into power supply systems. Rodriguez et al. [9] calculated

* Corresponding author.
E-mail address: hans-christian.gils@dlr.de (H.C. Gils).
[1] Current affiliation: AF Mercados EMI, Madrid, Spain.
[2] Current affiliation: 50Hertz Transmission GmbH, Berlin, Germany.

http://dx.doi.org/10.1016/j.energy.2017.01.115

Table 1
Variables used in the model description.

Symbol	Unit	Variable
$\boldsymbol{C}_{invest}$	k€/a	Annual depreciation of capital expenditure
$\boldsymbol{C}_{emission}$	k€/a	Emission certificate costs
$\boldsymbol{C}_{fuel}$	k€/a	Fuel costs
$\boldsymbol{C}_{unsupplPow}$	k€/a	Social welfare loss caused by unsupplied power demand
$\boldsymbol{C}_{operation}$	k€/a	Operation and maintenance costs
$\boldsymbol{P}_{addedCap}$	GW_{el}	Capacity of additional power plants or storage converter units
$\boldsymbol{P}_{addedLines}$	GW_{el}	Net transfer capacity of additional power transmission lines
$\boldsymbol{P}_{charge}(t)$	GW_{el}	Electricity storage energy input
$\boldsymbol{P}_{curtail}(t)$	GW_{el}	Curtailed power generation
$\boldsymbol{P}_{discharge}(t)$	GW_{el}	Electricity storage energy output
$\boldsymbol{P}_{export}(t)$	GW_{el}	Export power
$\boldsymbol{P}_{flow}(t)$	GW_{el}	Power flow over transmission lines
$\boldsymbol{P}_{gen}(t)$	GW_{el}	Power generation
$\boldsymbol{P}_{gridLoss}(t)$	GW_{el}	Power transmission losses
$\boldsymbol{P}_{import}(t)$	GW_{el}	Import power
$\boldsymbol{P}_{unsupplPow}(t)$	GW_{el}	Unsupplied power demand
$\boldsymbol{P}_{pump}(t)$	GW_{el}	Pumping power of reservoir hydro power plants
$\boldsymbol{Q}_{addedCap}(t)$	GW_{th}	Capacity of additional CSP solar fields
$\boldsymbol{Q}_{BUS}(t)$	GW_{th}	Thermal output of the CSP backup system
$\boldsymbol{Q}_{charge}(t)$	GW_{th}	Thermal storage energy input
$\boldsymbol{Q}_{discharge}(t)$	GW_{th}	Thermal storage energy output
$\boldsymbol{Q}_{SF}(t)$	GW_{th}	Thermal output of the solar field
$\boldsymbol{U}_{level}(t)$	GWh_{th}	Thermal storage filling level
$\boldsymbol{W}_{addedCapSt}$	GWh_{el}	Capacity of additional storage reservoir units
$\boldsymbol{W}_{level}(t)$	GWh_{el}	Electricity storage filling level

Table 2
Parameters used in the model description.

E_{annual}	GWh_{chem}	Annual resource/fuel availability
$Q_{existCap}$	GW_{th}	Installed solar field capacity
$P_{existCap}$	GW_{el}	Installed power plant or storage converter capacity
$P_{demand}(t)$	GW_{el}	Power demand
$P_{existLines}$	GW_{el}	Net transfer capacity of existing power transmission lines
$P_{inflow}(t)$	GW_{el}	Energy inflow to reservoir hydro power plants
P_{maxCap}	GW_{el}	Maximum installable power plant or storage converter capacity
$W_{existCapSt}$	GWh_{el}	Installed storage reservoir capacity
c_{OMFix}	%/a	Operation and maintenance fix costs
c_{OMVar}	k€/MWh	Operation and maintenance variable costs
$c_{specInv}$	k€/MW	Specific investment cost
$f_{annuity}$	–	Annuity factor
f_{avail}	–	Power plant availability factor
f_{cap}	–	Power plant capacity factor
f_{CCS}	–	Share of emissions that can be sequestrated
i	%	Discount rate
r_{S2W}	–	Solar to wind power generation ratio
$s_{gen}(t)$	–	Normalised profile of VRE resource availability
$s_{minFlow}$	–	Minimum outflow of hydro power plants
s_{VRE}	–	Theoretical VRE supply share
t_a	a	Amortization time
Δt	h	Calculation time interval
η_{charge}	$\frac{1}{100}$	Storage charging efficiency
$\eta_{discharge}$	$\frac{1}{100}$	Storage discharging efficiency
$\eta_{generator}$	$\frac{1}{100}$	Generator efficiency
η_{pump}	$\frac{1}{100}$	Pump efficiency
η_{self}	$\frac{1}{100}$	Storage self-discharging rate

backup energy, backup capacity, transmission capacity, and curtailed energy as technical parameters to be minimised in power systems with high VRE shares, and they calculated the resulting levelised costs of electricity for wind and photovoltaic shares as between 0% and 100%. They identified a VRE share of 50% with wind shares above 90% to be cost minimal and the system cost to be most dependent on the cost of wind turbines and backup energy. Dispatchable renewable power generation, i.e. hydro run-of-the-river, reservoir hydro, geothermal, and biomass power plants as well as storage were included in the backup capacity category; storage was not modelled as an explicit balancing option in their study. Jensen and Greiner [10] assessed the storage needs in highly renewable systems from a more fundamental perspective. Based on a time-series model of the storage filling level, they found a maximum storage demand at a VRE penetration of around 100%, with lower values reported at even higher VRE shares.

In purely economic approaches, system costs themselves are minimised, and cost minimal capacity expansion, dispatch, and the cost of system components are evaluated. Schaber et al. [11] calculated least-cost grid extensions for the expected power generation structure in Europe in 2020 and evaluated their effects on the supply system. They found that inadequate transmission capacities lead to high inequalities in Europe concerning utility revenues and that adequate international transmission grid extensions are advantageous for the base load as well as for VRE plant owners. In another publication, Schaber et al. [12] systematically assessed the grid integration costs for different VRE shares and mixes in Europe with the power demand at that time, assuming the following conditions: power generation capacities are distributed proportionally to the resource quality measured during full-load hours, 50% of the wind power capacity is offshore capacity, and pumped hydro storage is available through installations in 2012. Additional storage was excluded to concentrate on the integration effects and cost of the transmission grid.

These studies cover a wide parameter space. Nevertheless, many assumptions are made such as the distribution of power generation across countries and the technologies included or omitted. In particular, energy storage can interact with transmission and backup power generation. However, in Ref. [12], storage is 'assumed to remain at today's level' and in Ref. [9], storage is not included in investigated power systems. Considering storage as merely an option for backup power generation or a post-modelling option of excess energy consumption does not account for the interactions with other system components. Furthermore, the cited works use scenarios of predominantly national power generation infrastructure developments and do not consider the usage of concentrated solar power (CSP) technologies, which can provide dispatchable power production from an intermittent resource through thermal energy storage and conversion. Deployment of CSP technologies in regions with high direct insolation may change the need for the grid, storage, and backup capacities associated with solar power generation. In the present study, we investigate the need for balancing capacity and energy assuming an integrated market in Europe with competing and complementing balancing measures, allowing for storage expansion, optimising the geographical distribution of VRE capacities, and considering the potential of CSP as a renewable, dispatchable technology. We apply a linear, cost-minimising energy system model known as Renewable Energy Mix (REMix) to evaluate a set of scenarios with varying VRE shares and mixes in Europe. For each scenario, REMix performs an integrated optimisation of capacity expansion and hourly dispatch of power generation, storage and transmission. In addition to grid, storage, and backup capacity development, the following questions are evaluated for the outlined boundary conditions: How do overall power generation costs develop at high VRE shares and at different proportions of wind and solar power? How does VRE power generation interact with transmission, storage, and backup power generation? Of nuclear, fossil, CSP, biomass, and geothermal power plants, which technologies can provide backup at the lowest cost? To what extent are curtailments expected as an ultimate balancing

measure after transmission and storage?

The analysis is presented as follows. In Section 2, the REMix energy system model is introduced. The case study setup and input data are described in Sections 3 and 4, respectively. The results of the model application are presented in Section 5 and are discussed in Section 6. Finally, Section 7 summarises the conclusions that can be drawn from the case study.

2. Model description

REMix is composed of two main elements: the Energy Data Analysis Tool (REMix-EnDAT) and the Optimisation Model (REMix-OptiMo) (Fig. 1). REMix-EnDAT contains a global VRE resource assessment in high spatial and temporal resolution. It provides hourly generation profiles for the most important technologies aggregated to user-defined regions.[3] Furthermore, electricity and heat demand profiles are generated in that part of the model. The supply and demand profiles are input to REMix-OptiMo, which determines the least-cost operation of all system components during each hour of the year. This study focuses on the REMix-OptiMo modelling approach, which is described in detail in the following subsections.

2.1. REMix-OptiMo modelling approach

REMix-OptiMo is a deterministic linear optimisation program realized in a general algebraic modelling system (GAMS) formulation.[4] This approach was developed with the aim of providing a powerful tool for the layout and assessment of future energy supply scenarios based on system representation in high spatial and temporal resolution. The model is set up in a modular structure with a broad range of technology modules that are mostly independent of each other (Fig. 1). In each module, the parameters, variables, equations, and inequalities required for representation of the respective technical and economic characteristics are defined. Power generation, storage, and grid technologies are represented by their available and maximum installable capacity, investment, and operation costs as well as efficiency. All technology modules allow for technology dispatch and capacity expansion analyses. Expansion of power plants, transmission lines, or storage capacity can be optimised by the model according to the available potentials and system requirements. Investments in new capacities consider technology cost, amortization time, and interest rate, allowing for the calculation of proportional capital costs for the chosen optimisation interval.

REMix-OptiMo is a multi-node model. Demand and supply within predefined regions are aggregated to model nodes, which can be connected through electricity grids. Within the nodes, all generation units of each technology are grouped and treated as one single power producer. The model relies on a perfect foresight modelling approach and optimises over the overall time horizon, which is typically one year. This implies the assumption of a foreseeable future within the chosen optimisation interval and thus the negligence of forecasting uncertainty.

REMix-OptiMo is characterised by its objective function, boundary conditions, and constraints. The model variables include technology-specific power generation, power transmission, and storage in each time step and model region. If a capacity expansion is considered, additional variables reflect the model-endogenous installation of assets in each region. Constraints arise from technology-specific model equations and inequalities in addition to the power balance. The objective function that is minimised is the sum of the system costs in the overall investigation area. It is composed of the proportional investment and fixed operational costs of all endogenously installed system components for one year of their amortization time as well as the variable operational costs of all technologies.

The following paragraphs provide the modelling approach of the fundamental technology modules within REMix-OptiMo, which includes electricity demand, variable and dispatchable renewable power generation, conventional power generation, electricity-to-electricity storage, and direct current (DC) power transmission. Additional information on the modelling approach, model configuration, and further technology modules appears in Refs. [13,14,16,18].

In this work, model equations and inequalities are presented in simplified denotation. For better readability, the parameters and variables are displayed differently: variables are always written in bold font, and parameters appear in normal font. All model variables introduced in this chapter can have only positive values. For better readability of the model description, the corresponding boundary conditions are generally not included in the representation of equations. The same applies to the sets that parameters and variables are dependent on, which are generally model nodes, technologies, and the considered year.

2.2. Electricity demand

The electricity demand module provides the hourly electricity demand P_{demand} in each data node during one year. It is calculated from an annual demand and a normalised hourly load profile. The latter is obtained from historic data published by the European Network of Transmission System Operators [19] and is processed according to the methodology described in Ref. [14]. This module reflects the daily, weekly, and seasonal fluctuations in demand.

2.3. Power generation

For all power plant technologies, the hourly power generation $\boldsymbol{P}_{gen}$ is lower or equal to the installed and available net electric capacity. This includes an optional, exogenously defined existing capacity $P_{existCap}$ and the endogenous optimisation result $\boldsymbol{P}_{addedCap}$, as described by Eq. (1). Power plant outages are considered by the definition of an availability factor f_{avail}.

$$\boldsymbol{P}_{gen}(t) \overset{!}{\leq} \left(\boldsymbol{P}_{addedCap} + P_{existCap}\right) \cdot f_{avail} \qquad \forall t \tag{1}$$

The overall power plant capacity of each technology can be limited by a maximum value P_{maxCap} according to Eq. (2).

$$\boldsymbol{P}_{addedCap} + P_{existCap} \overset{!}{\leq} P_{maxCap} \tag{2}$$

The evaluation of costs with REMix-OptiMo considers capital cost $\boldsymbol{C}_{invest}$ and operational cost $\boldsymbol{C}_{operation}$. Capital cost is considered for all endogenously installed capacities $\boldsymbol{P}_{addedCap}$ and is calculated from the specific cost $c_{specInv}$, interest rate i, and amortization time t_a of the investment (Eqs. (3) and (4)). The annual operational cost includes a fixed and a variable element, which are proportionate to the capacity of newly installed units and to the annual power output, respectively (Eq. (5)). Depending on the technology, the latter may include variable production costs, fuel and CO_2

[3] Two separate implementations of REMix-EnDAT are available: a global inventory with a spatial resolution of 0.045° and historic data for 1984–2004 [13] and a European/North African inventory with a spatial resolution of 0.083°. and historic data for 2006–2014 [14,15]. This work relies on data from the latter implementation.

[4] This paragraph relies on previous publications [16,17].

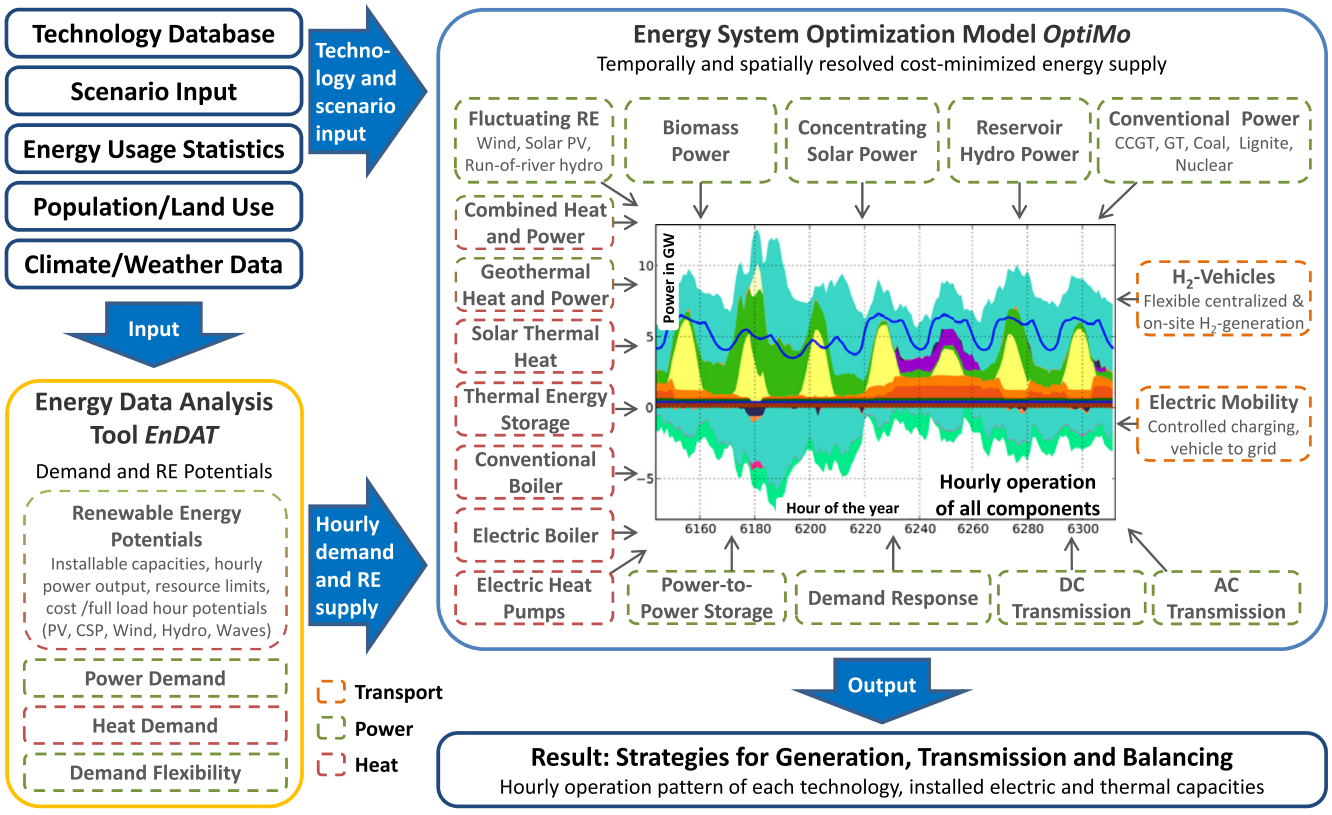

Fig. 1. REMix model components and structure, extracted from Ref. [16].

certificate costs.

$$f_{annuity} = \frac{i \cdot (1+i)^{t_a}}{(1+i)^{t_a} - 1} \tag{3}$$

$$\boldsymbol{C}_{invest} = \boldsymbol{P}_{addedCap} \cdot c_{specInv} \cdot f_{annuity} \tag{4}$$

$$\boldsymbol{C}_{operation} = \boldsymbol{P}_{addedCap} \cdot c_{specInv} \cdot c_{OMFix} + \sum_{t} \boldsymbol{P}_{gen}(t) \cdot c_{OMVar} \tag{5}$$

2.3.1. Variable renewable energy sources

Owing to their comparable characteristics, photovoltaic (PV) solar, run-of-the-river hydro and wind power are described by the same set of equations. The maximum hourly power output $\boldsymbol{P}_{gen}$ in each region is calculated from the corresponding installed and available capacity multiplied by a normalised profile s_{gen} of the resource availability. The latter is provided in REMix-EnDAT [13,14]. To account for the optional curtailment $\boldsymbol{P}_{curtail}$ of VRE power generation, Eq. (6) rather than Eq. (1) is applied.

$$\boldsymbol{P}_{gen}(t) + \boldsymbol{P}_{curtail}(t) \overset{!}{=} \left(\boldsymbol{P}_{addedCap} + P_{existCap}\right) \cdot s_{gen}(t) \qquad \forall t \tag{6}$$

The model-endogenous capacity expansion can be limited by the overall technology potential according to Eq. (2). For the calculation of capital and operational costs, Eqs. (4) and (5) are applied, respectively.

2.3.2. Reservoir hydro power

In contrast to run-of-the-river stations, reservoir hydroelectric power plants can provide both adjustable renewable electricity and storage. REMix-OptiMo considers all major plant components including the turbine, storage reservoir, and pump. Capacity expansion of turbines and pumps can be included in the assessment according to Eq. (2). The added turbine and pump capacities are independent of each other and are linked to the respective capital expenditures. Power generation and pumping are limited according to Eq. (1), with existing $P_{existCap}$ and added capacities $\boldsymbol{P}_{addedCap}$ regarding the turbines and pumps, respectively. An additional restriction in power generation can arise from the optional definition of a minimum turbine flow rate $s_{minFlow}$, which ensures that the downstream water resource availability is not adversely affected (Eq. (7)). The capacity factor f_{cap} represents the annual capacity utilization.

$$\boldsymbol{P}_{gen}(t) + \boldsymbol{P}_{curtail}(t) \overset{!}{\geq} \left(\boldsymbol{P}_{addedCap} + P_{existCap}\right) \cdot f_{cap} \cdot s_{minFlow} \qquad \forall t \tag{7}$$

The hourly water input, power generation, curtailment, pumping power, and change in storage level are linked by the storage balance according to Eq. (8). Similar to the calculation of VRE power generation, the natural inflow to the water reservoirs P_{inflow} is provided by REMix-EnDAT as an hourly time series. In all time steps, the storage level $\boldsymbol{W}_{level}$ is restricted to the overall storage capacity $W_{existCapSt}$, which is not subject to optimisation.

$$\left(P_{in\ flow}(t) + \boldsymbol{P}_{pump}(t) \cdot \eta_{pump} - \frac{\boldsymbol{P}_{gen}(t) + \boldsymbol{P}_{curtail}(t)}{\eta_{generator}}\right) \cdot \Delta t \overset{!}{=} \boldsymbol{W}_{level}(t) - \boldsymbol{W}_{level}(t-1) \qquad \forall t \tag{8}$$

Investment and operational costs of reservoir hydro stations are calculated according to Eqs. (4) and (5), respectively.

2.3.3. Concentrated solar power

CSP uses the energy of direct solar irradiation to heat the working fuel, which is then used for the production of steam for turbine operation. CSP plants can be equipped with thermal energy storage (TES) and backup firing systems (BUS), allowing for a dispatchable or even continuous power generation. In REMix-OptiMo, the installed capacities of all components can be either exogenously defined or optimised by the model. The overall solar field thermal capacity is composed of the exogenously defined existing capacity and the endogenously calculated added capacity and is limited to the overall potential according to Eq. (2). The solar field thermal output $\boldsymbol{Q}_{SF}$ arises from the overall capacity and the normalised hourly availability of the solar resource described by s_{gen}.

$$\boldsymbol{Q}_{SF}(t) \overset{!}{=} \left(\boldsymbol{Q}_{addedCap} + Q_{existCap}\right) \cdot s_{gen}(t) \qquad \forall t \tag{9}$$

The thermal balance of CSP plants relates the thermal output of a solar field $\boldsymbol{Q}_{SF}$ and backup unit $\boldsymbol{Q}_{BUS}$ as well as TES charging $\boldsymbol{Q}_{charge}$ and discharging $\boldsymbol{Q}_{discharge}$, with the power generation $\boldsymbol{P}_{gen}$ and curtailment $\boldsymbol{P}_{curtail}$ according to Eq. (10). The annual contribution of the BUS to the total thermal energy input can be restricted to any share of the solar field output.

$$\boldsymbol{Q}_{SF}(t) + \boldsymbol{Q}_{BUS}(t) + \boldsymbol{Q}_{discharge}(t) \overset{!}{=} \frac{\left(\boldsymbol{P}_{gen}(t) + \boldsymbol{P}_{curtail}(t)\right)}{\eta_{generator}} + \boldsymbol{Q}_{charge}(t) \quad \forall t \tag{10}$$

Hourly changes in TES energy level $\boldsymbol{U}_{level}$ are described by the storage balance, which accounts for charging, discharging, and self-discharging (Eq. (11)). An additional equation sets the storage level in the first and last time step to the same value, assuring that no energy is produced in the storage.

$$\left(\boldsymbol{Q}_{charge}(t) \cdot \eta_{charge} - \frac{\boldsymbol{Q}_{discharge}(t)}{\eta_{discharge}}\right) \cdot \Delta t - \frac{1}{2}\left(\cdot \boldsymbol{U}_{level}(t) + \boldsymbol{U}_{level}(t-1)\right) \cdot \eta_{self} \overset{!}{=} \boldsymbol{U}_{level}(t) - \boldsymbol{U}_{level}(t-1) \qquad \forall t \tag{11}$$

The hourly output of the power block $\boldsymbol{P}_{gen}(t)$ is limited by the available capacity as described by Eq. (2). Similarly, the storage level $\boldsymbol{U}_{level}$ must in all time steps be lower than the overall TES capacity. The CSP power generation cost is calculated according to Eqs. (4) and (5). Therein, the specific investment cost is considered separately for TES, BUS, and the power block.

2.3.4. Thermal power plants

Electricity production in thermal power plants can use geothermal energy, biomass, or conventional fuels. The latter include uranium and fossil fuels. In the model configuration applied in this work, thermal power stations are used exclusively to provide power. However, an alternative model representation accounting for combined heat and power generation is available in REMix [16]. The hourly output of conventional, biomass, and geothermal power plants is not dependent on a fluctuating resource but is restricted by the overall installed capacity according to Eq. (1). Technical restrictions in power plant ramping are not reflected in the model. In the cases of biomass and geothermal stations, the annual power generation might, however, be limited by the available resource E_{annual} (Eq. (12)).

$$\frac{\sum_t \boldsymbol{P}_{gen}(t)}{\eta_{generator}} \overset{!}{\leq} E_{annual} \tag{12}$$

The model-endogenous capacity expansion of thermal power plants can be constrained by the provision of maximum capacities according to Eq. (2). Costs are calculated according to Eqs. (4) and (5).

The fuel consumption of thermal power plants is obtained by dividing the power generation by the net efficiency. In the case of conventional power plants, it is used for calculating fuel cost $\boldsymbol{C}_{fuel}$, as well as CO_2 emissions and costs $\boldsymbol{C}_{emission}$. By defining a CCS factor f_{CCS}, the sequestrated share of CO_2 emissions can be defined.

2.4. Electric energy storage technologies

This module is designed to represent storage technologies with electric power input and output. The energy storage unit and converter unit are modelled separately in REMix-OptiMo. The central equation is the storage balance, which reflects all variations in the filling level. Analogous to the TES balance in CSP plants shown in Eq. (11), it ensures that in every time step, the change in storage level $\boldsymbol{W}_{level}$ equals the sum of storage input $\boldsymbol{P}_{charge}$, output $\boldsymbol{P}_{discharge}$, and self-discharge η_{self}. Losses occurring at charging (η_{charge}) or discharging ($\eta_{discharge}$) can be considered in the balance equation. As for TES, the storage level is set to identical values in the first and last time step by an additional equation. The storage filling level is limited by the installed storage capacity (Eq. (13)), whereas the power input and output are limited by the converter capacity analogous to Eq. (2).

$$\boldsymbol{W}_{level}(t) \overset{!}{\leq} \boldsymbol{W}_{addedCapSt} + W_{existCapSt} \qquad \forall t \tag{13}$$

The optimisation of storage capacities can be performed in two different modes, either with an exogenously defined ratio of storage to the converter unit or with an endogenous assessment of storage dimensioning. The technology module considers installation costs as well as fixed and variable operational costs of both storage and converter units. The latter is proportionate to the electricity charged into the storage.

2.5. Direct current power transmission

In this module, direct current (DC) power transmission technologies with different capacities and voltages can be implemented. Concerning costs and transmission losses, differentiation can be made between sea cables, underground cables, and overhead lines. High-voltage direct current (HVDC) interconnections and transmission capacities between model nodes can be user defined or endogenously added in the optimisation.

The power flow over each connection is limited by the overall capacity of the available lines. The corresponding Eq. (14) is applied to the power flow in both directions.

$$\boldsymbol{P}_{flow}(t) \overset{!}{\leq} \boldsymbol{P}_{addedLines} + P_{existLines} \qquad \forall t \tag{14}$$

Power transmission losses are considered on the basis of distances between the model nodes and increase linearly with the power transmission. The characteristic loss factor for each line is calculated from its length and the specific loss factors of power lines/cables on land, underwater cables, and converters. The installation cost is calculated for each line considering the lengths over land and sea as well as the number of converter stations.

2.6. Power balance, accounting, and objective function

The power balance in Eq. (15) for REMix-OptiMo ensures that at each model node and calculation time step, the power generation is

balanced with the corresponding demand. On the demand side, this includes hourly grid load P_{demand}, storage charging $\boldsymbol{P}_{charge}$, export $\boldsymbol{P}_{export}$, and grid losses $\boldsymbol{P}_{gridLoss}$. On the supply side, all types of power plant output $\boldsymbol{P}_{gen}$, storage discharge $\boldsymbol{P}_{discharge}$, import $\boldsymbol{P}_{import}$ and unsupplied power $\boldsymbol{P}_{unsupplPow}$ are included.

$$P_{demand}(t) + \boldsymbol{P}_{charge}(t) + \boldsymbol{P}_{export}(t) + \boldsymbol{P}_{gridLoss}(t) \stackrel{!}{=} \boldsymbol{P}_{gen}(t) + \boldsymbol{P}_{discharge}(t) + \boldsymbol{P}_{import}(t) + \boldsymbol{P}_{unsupplPow}(t) \qquad \forall t \tag{15}$$

The objective function to be minimised by REMix-OptiMo summarises the costs of all used technologies to the overall system costs. They arise from capacity expansion investment $\boldsymbol{C}_{invest}$, costs of operation $\boldsymbol{C}_{operation}$, fuel $\boldsymbol{C}_{fuel}$ and pollution $\boldsymbol{C}_{emission}$, as well as penalties for unsupplied power $\boldsymbol{C}_{unsupplPower}$.

$$\min\left\{\boldsymbol{C}_{unsupplPow} + \boldsymbol{C}_{invest} + \boldsymbol{C}_{operation} + \boldsymbol{C}_{fuel} + \boldsymbol{C}_{emission}\right\} \tag{16}$$

3. Case study structure

To study the correlation between VRE penetration, balancing power demand and supply costs, we considered a set of 19 scenarios differing in overall VRE share s_{VRE} and solar-to-wind ratio r_{S2W}. We defined the VRE share as a theoretical share that would be reached if no VRE power generation were curtailed or lost in storage and transmission. It is calculated as the proportion of wind and PV power in overall generation according to Eq. (17), where index i accounts for all considered generation technologies.

$$s_{VRE} = \frac{\sum_t \sum_{j \in Wind,PV} \left(\boldsymbol{P}_{gen,j}(t) + \boldsymbol{P}_{curtail,j}(t)\right)}{\sum_t \sum_i \left(\boldsymbol{P}_{gen,i}(t) + \boldsymbol{P}_{curtail,i}(t)\right)} \tag{17}$$

The solar-to-wind ratio r_{S2W} is calculated from the theoretical annual power generation of PV and wind according to Eq. (18). The contributions of onshore and offshore to overall wind power generation are subject to optimisation. In this work, we considered VRE shares of 0%, 20%, 40%, 60%, 80%, 100%, and 120%. For each VRE share greater than zero, three solar-to-wind ratios were assessed: 0.25, 1, and 4 which are equivalent to shares of 20–80, 50–50, and 80–20. The labelling of scenarios used hereinafter is composed of the VRE share followed by the technology shares, e.g. VRE20-S50W50 in the case of a 20% VRE share equally provided by solar and wind.

$$r_{S2W} = \frac{\sum_t \left(\boldsymbol{P}_{gen,PV}(t) + \boldsymbol{P}_{curtail,PV}(t)\right)}{\sum_t \left(\boldsymbol{P}_{gen,Wind}(t) + \boldsymbol{P}_{curtail,Wind}(t)\right)} \tag{18}$$

To evaluate power transmission, we subdivided the overall assessment area into 15 regions, as shown in Fig. 2 and Table 3. Power transmitted within regions was not considered, according to the 'copper plate' approach.

In addition to power generation shares, the model input includes capacity limits for renewable energy, transmission grids, and pumped hydro storage as well as fuel price, CO_2 emission certificate cost, and techno–economic parameters. These parameters are introduced in the following section.

The electricity supply optimisation case study presented in this work considers seventeen power generation technologies, seven electricity storage technologies, and one DC transmission technology. In addition to wind and PV, the model-endogenous capacity installation is considered for conventional, CSP, geothermal, and biomass power stations as well as for storage and transmission lines. On the contrary, the installed capacity of hydro power plants is exogenously defined. Considering the predefined VRE supply structure and technology parameters, the model evaluates the least-cost capacity expansion and operation of each technology. The system dispatch is optimised for 8760 time slices representing the hours of one year.

4. Model input data

REMix-OptiMo input includes technology characteristics as well as the regional values of power demand, renewable energy resources, and storage potential.

4.1. Power demand

The assumed annual power demand in the assessment area amounts to roughly 3650 TWh. It relies on the demand projection for the year 2050 in the Trans-CSP report [20], which provides a long-term power supply scenario for the EUMENA region composed of Europe, the Middle East, and North Africa. The annual demand is disaggregated to single hours of the year according to historic load profiles. These profiles were obtained by national transmission grid operators or were approximated by using publicly available data. An overview of the methodology and data sources was reported by Refs. [14,21]. By combining the projected annual demand with the historical profiles, the hourly load value range was determined to be 262–586 GW.

4.2. Power generation

The model configuration used in the case study considers ten renewable and seven conventional power generation technologies. Conventional power plants using fossil fuels or uranium can be installed with no limitations, whereas the usage of renewable energy technologies is restricted to the available potentials. By using high-resolution meteorological data as well as technology parameters, the potentials of biomass, geothermal, PV, CSP, and wind power are calculated in REMix-EnDAT [14]. Regarding hydro power, we assumed that the potential in Europe has been extensively exploited; thus, we did not allow for endogenous capacity expansion. However, we pre-set the installed capacities of the year 2010, which generates about 550 TWh/a of electricity, corresponding to about 15% of the total annual power demand. With an aggregated capacity of 193 GW, run-of-the-river and reservoir hydro stations can provide up to one-third of the annual peak load. The identified potentials as well as the installed hydro power generation

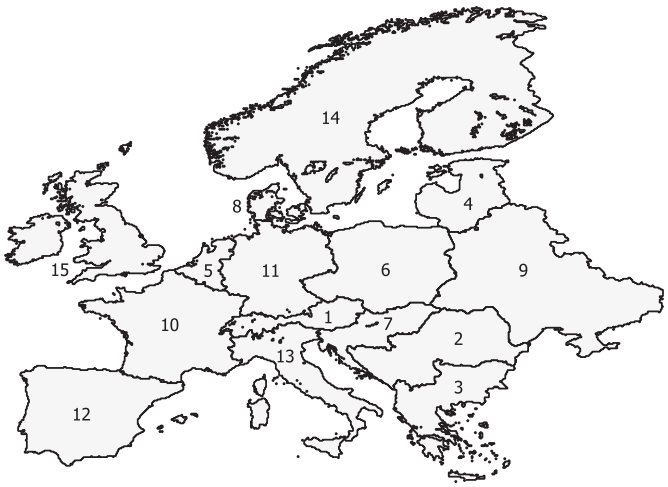

Fig. 2. REMix model regions considered in the case study.

Table 3
Countries included in each model region.

	Region	Countries included
1	Alps	Austria, Switzerland
2	BalkansNorth	Bosnia and Herzegovina, Romania, Serbia, Montenegro
3	BalkansSouth	Albania, Bulgaria, Greece, Macedonia
4	Baltic	Estonia, Latvia, Lithuania
5	BeNeLux	Belgium, Luxembourg, Netherlands
6	CentralEast	Czech Republic, Poland, Slovak Republic
7	CentralSouth	Croatia, Hungary, Slovenia
8	Denmark-W	Denmark West
9	East	Belarus, Moldova, Ukraine
10	France	France
11	Germany	Germany
12	Iberia	Portugal, Spain
13	Italy	Italy
14	Nordel	Denmark East, Finland, Norway, Sweden
15	UK-IE	Ireland, United Kingdom

capacities in each region are summarised in Table 4 in the Appendix.

The power generation of solar, wind, and hydro power is given by the availability of the intermittent resources. For each technology and geographical region, hourly generation profiles are also determined by REMix-EnDAT. The generation profiles applied in this work rely on data for the year 2006 and represent the average availability compared with other recent meteorological years [15].

To evaluate the benefits of TES availability, we accounted for three CSP configurations reflecting different solar multiples and thus operation patterns. The solar multiple is defined as the ratio of the thermal output from the solar field against the thermal input of the steam turbine. The configuration *CSP-base* has a solar multiple of 3.5 and represents a technology for base load power provision. To decouple the power production from solar irradiation, the CSP plant is equipped with a TES dimensioned to supply 18 h of full-load turbine operation. The configurations *CSP-mid* and *CSP-peak* are designed with lower solar multiples of 2.5 and 1 and are equipped with TES allowing for twelve and six hours, respectively. For the provision of firm capacity, all CSP plants use natural gas-fired backup systems allowing for full-load power block operation.

The most important techno–economic parameters of all power generation technologies are summarised in Table 5. They reflect significant technology cost reductions, especially for wind power, PV, CSP, CCS, and storage, which are assumed to be achieved through technological learning in the future. Further parameters include TES charging and discharging efficiencies of CSP plants $\eta_{charge} = \eta_{discharge} = 95\%$, the CCS factor $f_{CCS} = 0.9$ describing the share of emissions that can be sequestrated, and the minimum flow rate of reservoir hydro stations $s_{minFlow} = 0.25$. For the fuel costs, we assumed values of 2.5 €/GJ for coal, 8 €/GJ for natural gas, 2 €/GJ for uranium, and 10 €/GJ for biomass. Considering the existence of an effective CO_2 emission trading system, we applied emission certificate costs of 150 € per tons of CO_2. All investments in new power generation, storage, or grid technologies are subject to a fixed capital interest rate of 6%.

4.3. Electric energy storage

The case study considered three different storage technologies: redox flow battery (RFB), pumped storage hydro (PSH), and hydrogen storage. RFB and hydrogen tanks were chosen as representatives for short- and long-term storage technologies, respectively, which are not subject to direct limitations in resource availability. To consider different storage designs, three configurations each of RFB and hydrogen storage were included. RFB can be installed with the ratio r_{S2C} of storage to converter units of 4 h, 7 h, and 24 h and hydrogen storage with 100 h, 400 h, and 800 h. For PSH, we assumed that the storage reservoir capacity of the year 2010 will persist but cannot be extended. To be used, it must be complemented by a model-endogenous installation/refurbishment of converters with an upper limit corresponding to the converter capacities of the year 2010. Table 6 in the Appendix summarises the techno–economic storage parameter applied in this work. To account for the limited geographic availability of hydrogen caverns, the cost of hydrogen storage represents a mixture of caverns and the globally available technology of hydrogen tanks.

4.4. Power transmission

Grid capacity expansion is limited to point-to-point HVDC connections between neighbouring model regions with a maximum capacity of 30 GW. According to [20], we assumed transmission power losses of 0.45%/100 km on land and 0.27%/100 km in sea cables. An additional 0.7% is lost in each converter station. Investment costs differ substantially between overhead lines and sea cables; here, values of 490 k€/km and 1950 k€/km were applied, respectively. Additional costs of 162000 k€ arose from the installation of each converter station. We assumed an amortization time of 40 years and annual fixed operational costs equivalent to 0.6% of the investment [20]. The distances between the considered model regions are listed in Table 7 in the Appendix.

5. Results

The model results provide insight into the least-cost capacity installation and operation of all system components. Depending on the applied VRE share s_{VRE} and solar-to-wind ratio r_{S2W}, different system configurations and electricity supply costs are determined.

5.1. Power generation

The overall power generation was 3675–3903 TWh. Owing to losses in storage and transmission, it exceeds the demand projection by a maximum of 7%. Losses increase with VRE share and are highest in supply systems dominated by PV. The allocation of these losses to storage and grid is presented in Sections 5.2 and 5.3, respectively. The dynamics of the technology dispatch resulting from the objective function Eq. (16) and the scenario assumptions is exemplarily shown in Fig. 3.

5.1.1. Biomass, geothermal, and hydro power

According to the REMix results, biomass and geothermal power plants were not installed in any scenario. This implies that with the cost assumptions applied here, they are not competitive with alternative technologies.

In contrast and owing to the consideration of the current power plant capacities, hydro power contributed substantially to the power supply. The annual power generation differed little between the scenarios, ranging from 515 TWh in the scenarios with the highest $s_{V\,RE}$ values to 585 TWh in those with lowest $s_{V\,RE}$; this is equivalent to a generation share of 14%–16%. Therefore, the net contributions of VRE and conventional technologies to the overall supply did not exceed 86%.

5.1.2. PV and wind power

PV and wind generation are determined mostly by the scenario input. However, because their fluctuating nature causes curtailments in peak production hours and hydro power stations operate at zero marginal costs, their net output did not reach the predefined supply shares (Fig. 4). Curtailments were generally higher in scenarios dominated by PV (Fig. 7). Overall, the VRE capacities were

about 120–3070 GW for PV and 46–1330 GW for wind power. Analysis of the regional REMix results revealed that good wind onshore potentials in coastal regions were exploited first. For wind generation shares exceeding roughly 30%, they were complemented by offshore wind power. Across all scenarios, wind power was installed mostly onshore; the offshore share in total wind capacity reached a maximum of 32% (Fig. 4).

5.1.3. Concentrated solar power

The exploitation of CSP potentials was highest in the scenario without VRE and decreased with the VRE share. The overall capacities were between 92 GW in VRE0 and 0 GW in scenarios with 120% VRE share as well as in VRE100-S20W80 and VRE100-S50W50. With an increase in VRE share, wind power and PV gradually reduced the annual full-load hours of the CSP plants, which were no longer competitive with the gas-fired power plants when values below 4000 h/a were reached; the maximum values were 4270–4570 h/a for CSP-mid and 5380 h/a for CSP-base. At VRE shares of 40% and greater, this effect became particularly important in scenarios considering a PV-dominated VRE mix.

Of the three available configurations, mostly CSP-mid was used. The only exception was scenario VRE0, in which 19 GW of the configuration CSP-base was built. In this scenario with no PV, CSP was used throughout the day, with a focus on the provision of medium-load coverage during the day and in the evening and morning hours. With an increasing amount of PV entering the system, the operation of CSP increasingly shifted to evening and night times, which made the CSP-mid configuration more competitive. The overall power generation in CSP was between 420 TWh, or approximately 11.5% of the overall generation, in scenario VRE0 and 11 TWh in VRE100-S80W20.

5.1.4. Conventional power plants

Across all scenarios, renewable energy technologies were complemented by conventional power plants. Their overall gross capacities were between 132 GW in scenario VRE120-S20W80 and 530 GW in scenario VRE0, which is equivalent to 22% and 90% of the annual peak load, respectively (Fig. 5). Three technologies were not used in any scenario: nuclear power plants, coal power plants without CCS, and gas turbines with CCS. Coal power plants with CCS were the dominant technology at VRE shares below 40% but were not used at theoretical VRE shares of more than 80%. In contrast, gas-fired power plants were used across all scenarios, with an aggregated capacity of 132–244 GW. The gradual reduction of coal power plant capacity with increasing VRE share originates from the same phenomenon as that of CSP capacity: at lower annual full-load hours, specific generation costs of backup technologies are increasingly dominated by fixed instead of variable costs, favouring those technologies with lower investment cost. In scenarios dominated by wind power, mostly gas turbines were installed, whereas in those with a balanced mix or high PV share, CCGT was preferred. The CCS share in the power plant park was highest in scenario VRE0 and decreased with the VRE share. This decrease was significantly more pronounced in scenarios dominated by wind power. At the highest VRE shares, no power plants with CCS were installed in scenarios VRE100-S20W80, VRE120-S20W80, and VRE120-S50W50. In contrast, 22% of the conventional power plants in VRE120-S80W20 had CCS technology.

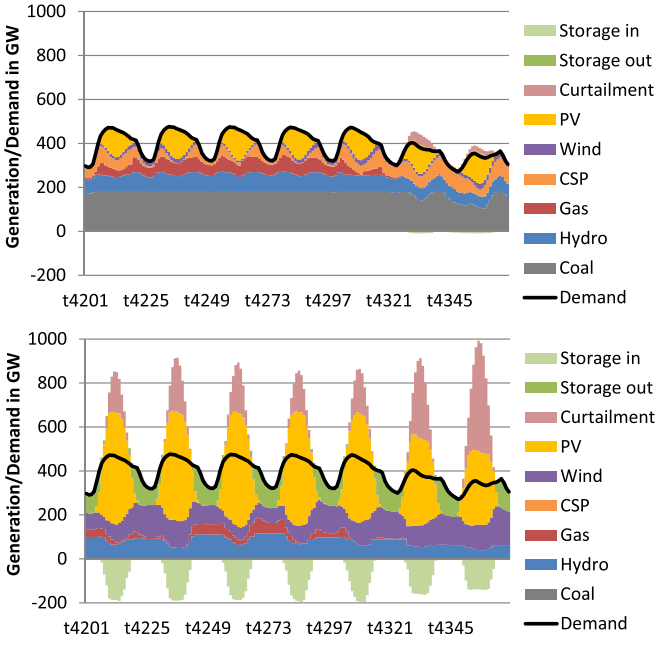

Fig. 3. Power generation dispatch in a summer week in scenario VRE20-S50W50 (above) and scenario VRE100-S50W50 (below).

The share of conventional power plants in the overall power generation was between 1% in scenario VRE120-S20W80 and 73% in VRE0. A comparison of different mixes of solar and wind power revealed that less conventional generation is needed for those dominated by wind power and more is required for those dominated by solar power. The decrease in conventional generation that can be achieved by a 20% increase in VRE was reduced from an average of 17% for VRE shares of up to 60% to an average of 2% for a 120% VRE share. This can be explained by the fact that in the hours in which the VRE generation exceeds demand already at low VRE shares, no further substitution of backup generation can be achieved by adding more VRE capacity. With an increase in VRE share, this occurs in more hours.

The share of CCS in overall conventional generation exceeded 85% for VRE shares of up to 60%. For higher VRE shares, it rapidly declined for wind-dominated and balanced supply mixes and remained at more than 45% for solar-dominated mixes.

5.1.5. Regional power generation

Owing to the strong differences in both the quantity and quality of VRE potentials, the regional power generation is to a high degree influenced by the predefined wind and solar shares, as shown in shown in Fig. 6 for the scenarios dominated by wind and PV, respectively. At high wind supply shares, the regions of Denmark-W, Nordel, and UK-IE became major exporters, whereas Germany, France, CentralEast, CentralSouth, and BalkansNorth imported significant shares of their demand. On the contrary, in solar-dominated scenarios, BalkansSouth, Iberia, Italy, and Alps provided electricity mostly to East, Germany, BalkansNorth, and BeNeLux. The regional generation patterns for the balanced supply mix are similar to those in wind-dominated cases, albeit with less wind surplus in Denmark and UK-IE, at the expense of more solar generation in southern Europe. In the scenario without VRE, the net import amounts were negligible for all regions except France, which imported about 4% of its demand from the Alps region, Germany, and the British Isles.

5.1.6. Availability of firm generation capacity

Firm generation capacity can be provided by all technologies that can store their fuel or working media. This implies that their availability for power generation does not depend on a highly fluctuating resource. The availability of VRE generation in the peak load hour can be assessed by comparing the sum of year-round available firm capacities of conventional, reservoir hydro, and CSP plants as well as storage to the annual peak load. Considering the power plant availabilities and efficiencies listed in Table 5, we

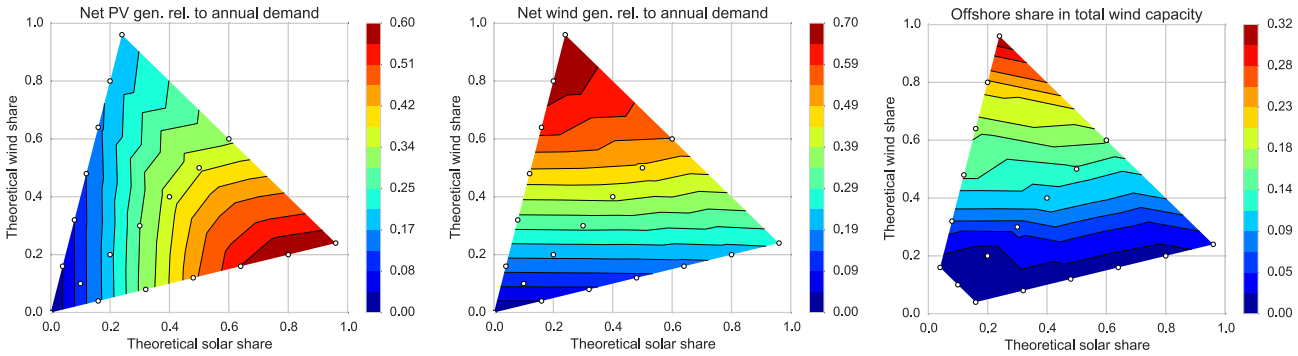

Fig. 4. Variable renewable energy (VRE) supply structure showing (left to right) net photovoltaic (PV) generation, net wind generation, and offshore share in overall wind turbine capacity. The white dots represent the scenarios optimised in REMix.

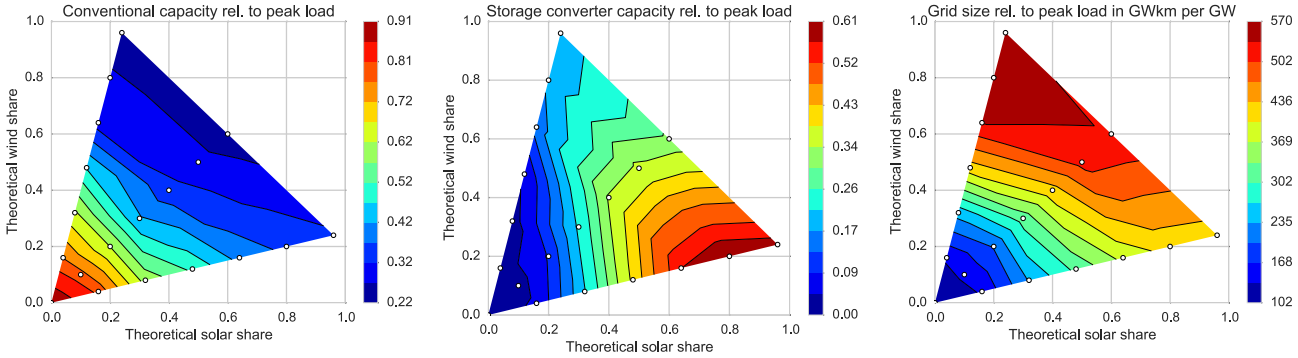

Fig. 5. System characteristics depending on theoretical solar and wind shares including (from left to right) backup and storage converter capacity in GW/GW_{peak} and grid size in GWkm/GW_{peak}. The white dots represent the scenarios optimised in REMix.

determined ratios of firm capacity to peak load between 32% and 95% for VRE120-S20W80 and VRE0, respectively. Furthermore, the available storage capacities were between 0.4% (VRE0) and 59% (VRE100-S80-W20) of the peak load. It appears that the gap between peak load and firm generation capacity was highest in the wind-dominated scenarios, reaching up to 50% at 120% VRE. For a balanced supply mix, the maximum value amounted to 36% at 120% VRE, whereas it did not exceed 10% in the solar-dominated scenarios. These results reflect a high availability of wind power and a low availability of solar PV in peak load hours. The identified capacity gaps can be filled at least partially by run-of-the-river hydro stations, which provide 11% or more of the peak load during every hour of the year.

5.2. Electric energy storage

The model-endogenous capacity expansion of PSH converters amounted to values between 2 GW in scenario VRE0 and 32 GW in VRE60-S50W50, which is equivalent to 0.4% and 5.5% of the annual peak load, respectively. Independent of the VRE share, the values were highest in solar-dominated systems and lowest in wind-dominated systems. The same applies to the installation of battery storage capacities, which were between 0 GW in VRE20-S20W80 and 322 GW in VRE100-S80W20. The corresponding energy capacity reached up to 2 TWh. At low VRE shares, battery storage is built only with the lowest available energy-to-power ratio of four hours; at more than 60% VRE, the energy-to-power ratio of 7 h was also used. In this way, the shifting of mostly solar generation to the night hours can be extended. Hydrogen storage was used in only one scenario, VRE80-S20W80, in which capacities of 21 GW and 3.1 TWh were installed.

The aggregated converter capacity of all storage technologies reached up to 352 GW or 60% of the annual peak load (Fig. 5). A comparison of the storage energy capacity with the average daily electricity demand revealed that the highest values of more than 20% were attained for battery storage. The predefined PSH reservoirs allow for storage of about 3%, whereas the hydrogen storage in scenario VRE80-S20W80 is dimensioned to store 31% of the average daily demand.

The annual storage output amounted to values between 5 TWh and 742 TWh, which is equivalent to 0.15% and 20% of the annual power demand, respectively. The values generally increased for higher VRE and in particular, PV shares (Fig. 7). The corresponding storage losses accounted for 0.04%–4.8% of the annual demand (Fig. 7).

5.3. Power transmission

The model-endogenous grid installation amounted to an overall capacity of 60 TWkm–331 TWkm, which increased with VRE share and with the contribution of wind power in particular. By relating the grid capacity and annual peak load, specific values of 102 GWkm/GW–564 GWkm/GW were obtained. The annual power transmission ranged from 6% of the annual demand in scenario VRE0 to 30% in VRE120-S20W80. With the exception of those with 40% VRE or less, the share of transmitted energy was always highest in scenarios dominated by wind power, followed by those dominated by solar power. Owing to the consideration of low-loss HVDC technology and the negligence of all lower grid levels, the transmission losses were found to be lower than the storage losses. Values between 16 TWh and 76 TWh were reached, which is equivalent to 0.4% and 2.1% of the annual demand, respectively. Compared with the transmitted energy, the grid losses were between 6.4% and 8.2%.

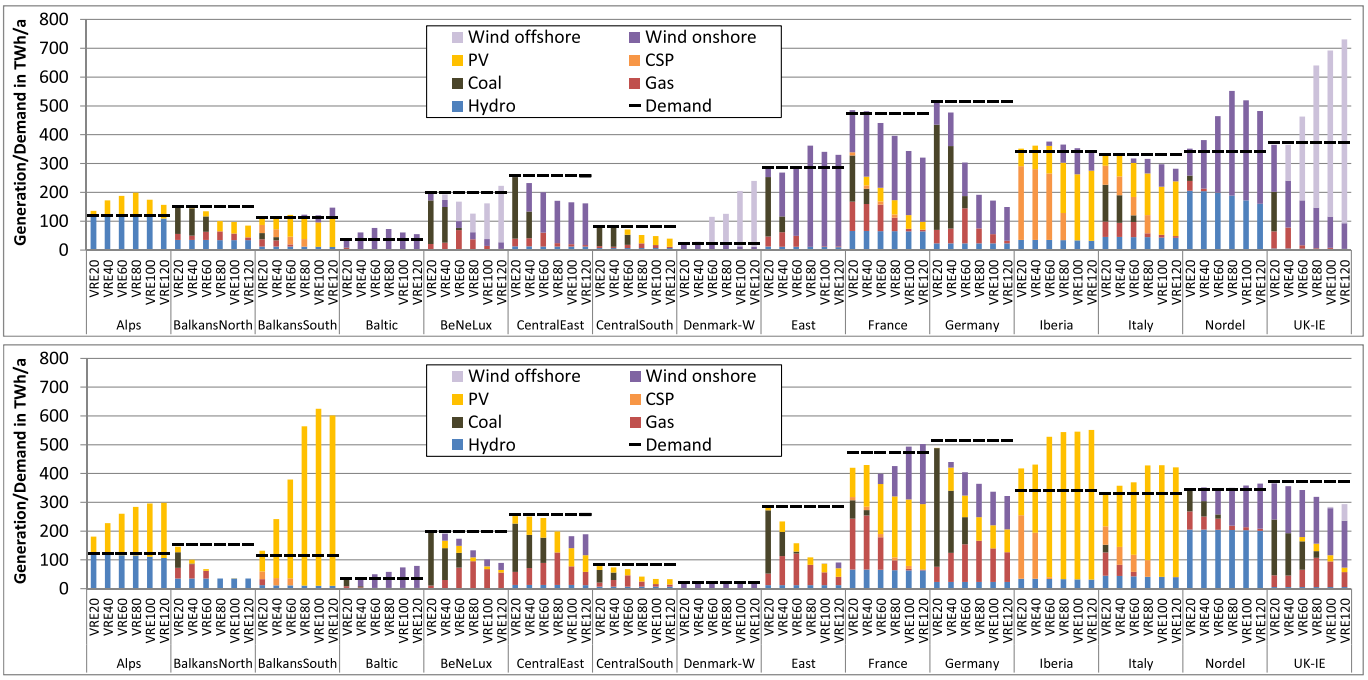

Fig. 6. Regional power generation and annual demand in scenarios dominated by wind (above) and solar power (below).

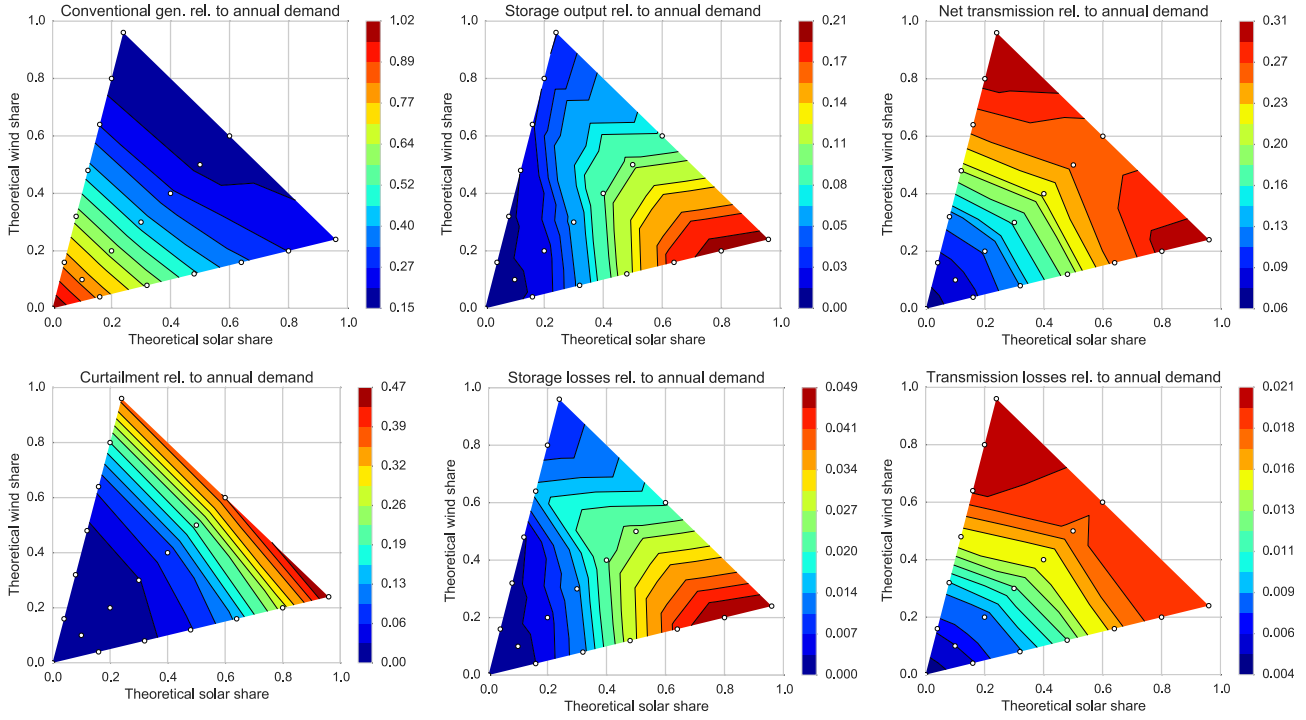

Fig. 7. System operation characteristics depending on theoretical solar and wind shares. Images from left to right and top to bottom show backup generation, storage output, import after transmission loss, curtailment, storage loss, and transmission loss relative to the annual electricity demand. The white dots represent the scenarios optimised in REMix.

5.4. *Levelised cost of electricity*

Fig. 8 indicates the levelised cost of electricity (LCOE), which is calculated by dividing the total system cost by the total annual power demand. The total system LCOE was between 0.088 €/kWh and 0.121 €/kWh. These values were generally higher in solar-dominated systems, whereas those for wind-dominated systems and systems with equal shares differed little. The minimum system LCOE occurred at 20% VRE penetration in solar-dominated systems (0.094 €/kWh), 40% VRE penetration in systems with equal shares of wind and solar power (0.091 €/kWh), and 60% VRE penetration in wind-dominated systems (0.088 €/kWh). These costs also accounted for annuities of the considered reservoir and run-of-the-river hydro power plants as well as pumped storage hydro reservoirs, which were not included in the optimisation. If emission costs were not regarded, the cost minima occurred at lower VRE

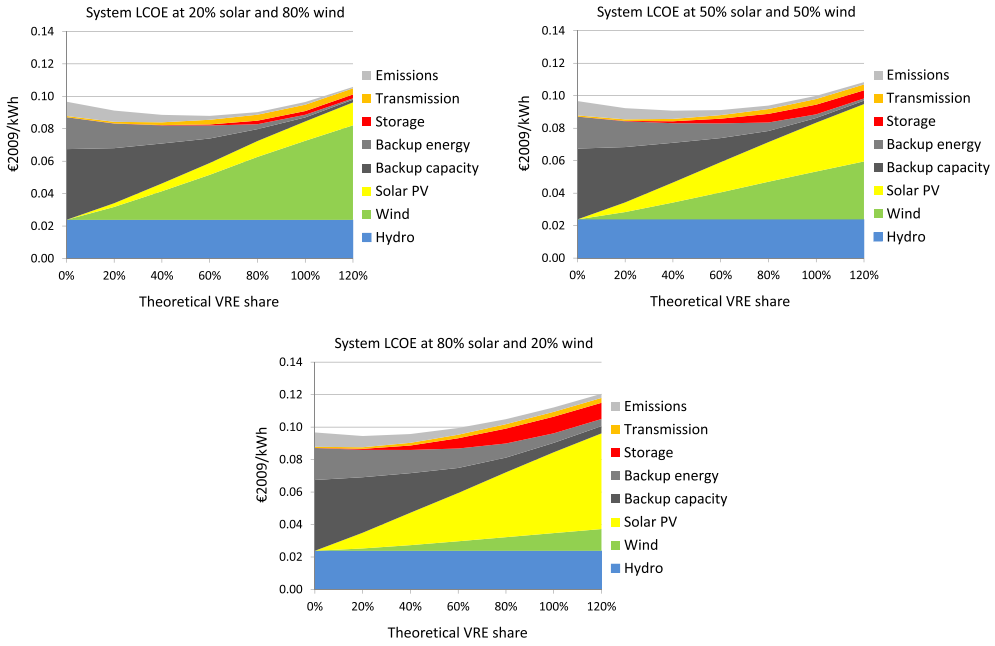

Fig. 8. Structure of system levelised cost of electricity (LCOE) showing the proportions of costs for power generation, storage, transmission, and CO_2 emissions. The panels at upper left show scenarios with 20% photovoltaic (PV) and 80% wind; those at upper right show scenarios with 50% PV and 50% wind; and the bottom panels show scenarios with 80% PV and 20% wind.

shares, at 40% in wind-dominated scenarios and 20% in solar-dominated and balanced scenarios.

According to the REMix results, the solar-to-wind ratio had only a limited effect on the overall system LCOE. A comparison of scenarios with the same VRE share revealed that the differences between the wind-dominated and solar-dominated cases did not exceed 16%, which is equivalent to 0.016 €/kWh. The impact of the supply mix on LCOE increased with the VRE share, with a maximum occurring at 100%. The LCOE values in wind-dominated and balanced scenarios differed by a maximum of 4% (0.004 €/kWh).

The costs for VRE power generation contributed up to 68% of the total system LCOE. The solar-to-wind ratio changed this contribution only by up to 0.001 €/kWh. This implies that the differences in cost are due mostly to the balancing infrastructure. Above 60% VRE share, the VRE power generation costs were higher for wind-dominated systems than for solar-dominated systems. Nevertheless, the total system LCOE were lower in the wind-dominated systems because solar power induces mostly higher integration costs, especially for storage, backup capacity, and backup energy. At maximum, storage accounted for 9% of the system LCOE. The maximum share of transmission in the system LCOE amounted to 4%. Hydro power accounted for 20%–27% of the system LCOE.

5.5. Sensitivity to input variations

To test the sensitivity of the results to variations in the most important input parameters, several additional model runs were performed for particular scenarios. These runs focused on investment costs of storage, grid, and backup technologies as well as hourly availability of wind and solar power. For battery storage, both an increase and decrease in investment costs by 50% were

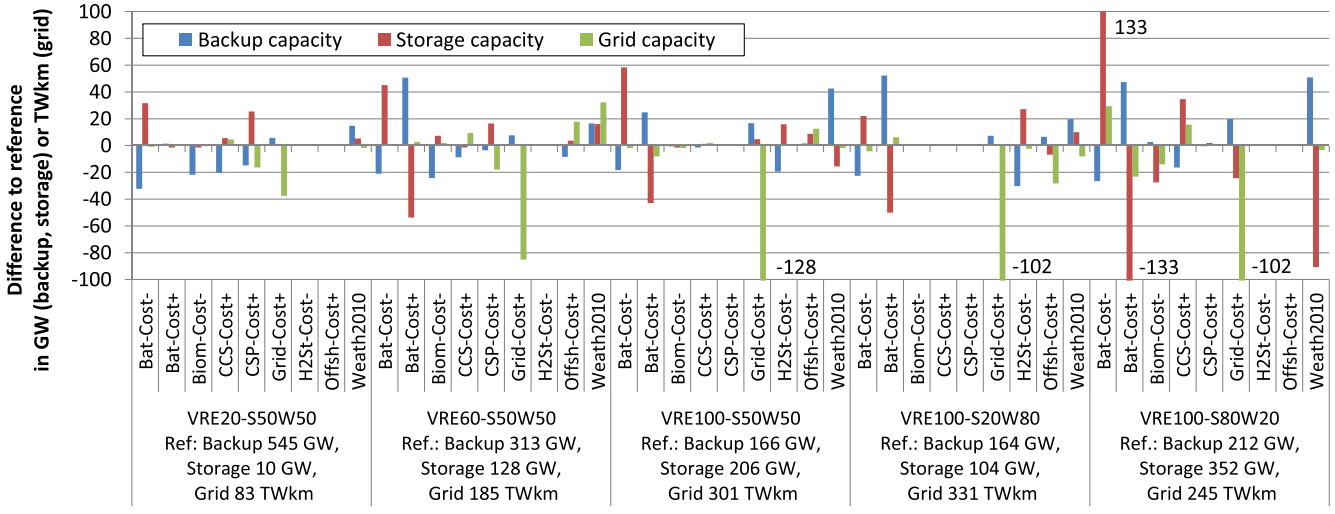

Fig. 9. Impact of the input variations on the demand for backup, storage and grid capacities. The reference values are included in the corresponding scenario labels. Higher and lower battery costs are assessed in Bat-Cost+ and Bat-Cost-, respectively, lower biomass fuel costs in Biom-Cost-, higher CSP, CCS and grid costs in CSP-Cost+, CCS-Cost+ and Grid-Cost+, respectively, lower hydrogen storage costs in H2St-Cost-, higher offshore wind costs in Offsh-Cost+, and different VRE and demand time series in Weath2010.

considered. Assuming that underground caverns can be used, the investment cost of hydrogen storage reservoirs was reduced by 90%. Because hydrogen storage was used in only one of the scenarios, the impact of higher cost was not evaluated. Grid investment cost is an additional sensitivity concern. Rather than overhead lines, we considered underground cables with an investment cost of 1661 k€/km and a specific loss of 0.34%/100 km. The costs of power generation technologies were modified in four ways: a reduction of biomass fuel cost by 50%, an increase in CCS investment cost by 100%, an increase in offshore wind investment cost by 50%, and an increase of CSP solar field and thermal storage investment costs by 50%. Finally, we evaluated the impact of different solar irradiation, wind speed, and demand time series. Here, historic data of the year 2010 were used, reflecting a year with considerably lower PV and wind generation availability at approximately −6% for wind offshore, −14% for wind onshore, and −6% for PV. All variations were applied to scenarios VRE20-S50W50, VRE60-S50W50, VRE100-S50W50, VRE100-S20W80, and VRE100-S80W20.

The REMix results showed that all considered parameter variations had significant impacts on the system composition and operation. Changes in backup technology costs including CSP, CCS, and biomass were the most effective at low VRE shares of 20% and 60%, whereas those affecting storage and grid costs were more influential at 100% VRE (Fig. 9). At lower fuel costs, biomass substituted up to 50% (130 GW) of the conventional capacity and up to 70% (750 TWh) of conventional generation, enabling an emission reduction of up to 40%. The assumption of 50% higher investment cost almost completely eliminated CSP from the system; solar power was substituted by short-term storage and conventional generation, causing an increase in emissions of up to 17%. Higher CCS cost caused a technology shift to non-CCS fossils and CSP, which correlates with a maximum increase in emissions by a factor of 2. Higher grid cost reduced transmission capacity and power transmission by 44% (175 GWkm/GW_{peak}) and 38% (300 TWh), respectively, which was compensated mostly by additional conventional capacity and generation. Its impact increased with the VRE share and was particularly high in the wind-dominated scenario. Different battery costs mostly affected the usage of batteries and conventional power plants at high VRE and PV shares in particular. At lower costs, up to 30% (110 TWh) of conventional generation was substituted by storage, whereas at higher costs, it increased by up to 40% (175 TWh). The consideration of significantly lower reservoir costs brought hydrogen storage into the scenarios with highest wind shares. Installed capacities reached 18 GW/12 TWh at 50% and 27 GW/11 TWh at 80% wind supply share and enabled the substitution of 45 TWh (25%) and 50 TWh (50%) of conventional generation, respectively. Higher offshore wind costs led to a shift towards onshore wind power, which correlates with higher generation capacity and a reduction in conventional power generation. The consideration of 2010 weather data caused significant increases in backup capacity demand and conventional generation by up to 25% (50 GW) and 60% (250 TWh), respectively. The impact of different time series increased particularly with the PV supply share. The impact of lower or higher emission cost was evaluated in a comparable scenario study based on REMix [22], which showed that the composition of the conventional backup capacity was mainly influenced and that hydrogen storage became more relevant at higher emission costs.

Even though the system composition and operation were found to be highly dependent on single cost parameters, the overall system cost was affected to a much lower degree. At 100% VRE share, the modifications of CCS, CSP, biomass, and hydrogen storage did not change the overall cost by more than 0.5%. Instead, halved or doubled battery costs caused a decrease and increase of 1%–5% each. More importantly, the assumption of higher grid cost or lower VRE full-load hours lead to overall cost increases of 3%–6%. The highest impact was found for the assumption of higher offshore wind costs in the scenario with 80% wind power supply, which amounted to a cost increase of almost 11%. At lower VRE shares (20% and 60%), a different result was noted. There, higher offshore wind or lower hydrogen storage cost did not have a notable impact on the supply cost. The variation in battery and CSP costs caused changes in overall costs by less than 2%; those concerning biomass and grid costs changed less than 3%. Most significant were the cost increases of 7% caused by higher CCS costs in the 20% VRE scenario and 6% caused by less PV and wind power generation in the 60% VRE scenario.

6. Discussion

The REMix energy system model was designed to analyse the integration of renewable energy into power systems. REMix provides several important benefits over other such models. Firstly, its approach involves a deterministic optimisation of the operation and the capacity expansion of all modelled technologies. In addition, REMix optimises over the overall time horizon of one year in hourly resolution rather than considering only selected time periods. Another outstanding characteristic of the model concerns the global renewable energy resource assessment in high spatial and temporal resolution. REMix is therefore especially apt for analysing VRE power generation effects on a residual system, such as backup, transmission, and storage capacity expansion and utilization, curtailments, and other losses as well as supply costs. In contrast to other energy system models, REMix does not consider the complete energy system; rather, it focuses on the power sector.

The intended approach for the model case study presented here is a systematic comparison of a wide variety of energy scenarios for Europe in which the model behaviour depends on different assumptions. To maintain the model complexity and computation time low, we used a rather simplified and schematic representation of the power system. This allows us to identify individual interrelations between VRE technologies and other elements of the power system. The model results primarily give insight into the nature and function of REMix and provided essential new findings relevant for the transformation of energy supply systems. Of particular importance were those regarding the role of different storage technologies and CSP as options for providing firm capacity from solar energy.

Important approximations of the model as introduced and applied in this study are the assumption of unrestricted 'copper plate' transmission within large model regions and the negligence of technical flexibility restrictions such as ramping or partial load constraints for thermal power plants. The copper plate assumption neglects grid costs on lower voltage levels. Distribution grid extensions or additional local storage might be necessary to compensate for fluctuations and losses on the local scale, thus leading to higher costs and possibly different system structures than those calculated by REMix. Consideration of the flexibility restrictions in conventional power plants might also alter the modelling results, especially the structure of the backup power provision. The consideration of balancing measures alternatively or in addition to the selected storage and transmission technologies might also change the case study outcome. Other REMix studies that focus on Germany have assessed the impact of controlled battery electric vehicle charging and vehicle to grid technologies [23], demand response [17], and enhanced coupling between electricity and heating sectors [16,21]. Such studies have shown that all of these technologies can provide balancing power and energy at lower costs than those related to backup power plants.

This implies that their consideration in future modelling studies can further reduce the supply costs calculated in this work.

Compared with previous studies with a similar scope, the major novelty of our work lies in the consideration of storage capacity expansion, dispatchable CSP plants, and regional technology potentials. Except for hydro power, all generation, storage, and transmission capacities are subject to optimisation. Assuming the current hydro power capacities, the effective supply share of all other technologies is limited to approximately 86%. When considering these capacities, we did not assess whether the substitution of hydro power by wind and PV might be more economic than the replacement of these units at the end of their lifetimes. However, such replacement is expected to be less costly than the installation of new units.

The results of the case study showed that the predefined solar-to-wind ratios have significant impact on the choice of balancing technologies. In systems dominated by solar PV, the balancing of fluctuations was mostly provided by short-term storage and CCGT, whereas wind power was preferably combined with gas turbines, CSP, power transmission, and in some cases long-term storage. This behaviour can be explained by the typical fluctuation pattern of VRE technologies. The model-endogenous installation of storage and transmission lines increased with the VRE share, whereas that of the conventional backup capacity decreased. The corresponding decreases in conventional power generation were even more pronounced, which implies a gradual reduction in annual full-load hours for the remaining capacities, causing a technology shift from coal to CCGT and then to gas turbines.

The evaluation of firm generation capacity indicates the extent to which generation capacity might be needed, in addition to the system configuration determined by REMix, to ensure security of supply. Assuming zero power generation from variable resources, additional generation or storage capacity of up to 50% of the peak load can be required. By the output of run-of-the-river hydro stations, this value can be reduced to 39% at most. Considering the historical weather data of 1984–2004, the REMix-EnDAT global resource assessment tool indicates that the annual minimum wind power generation in the overall assessment area was 2.8%–7.2% of the installable capacity for onshore turbines and 2.6%–9% for that of offshore turbines. This can be considered as a rather pessimistic estimate for minimum wind generation because all available turbine sites were included, whereas the deployment in REMix was concentrated in the regions with highest availability. Considering the 21-year minimum values, the remaining supply gap reaches more than 10% of the peak load in all scenarios with theoretical wind supply shares of 45% or more and peaks at 32% of the peak load at almost 100% wind share. It follows that in order to ensure complete load coverage also in the case of a coincidence of peak load and minimum wind supply, approximately 200 GW of additional generation capacity is required. Applying the cost of gas turbines, this would more than double the back-up capacity cost. Considering their limited contribution to the overall system cost, this would, however, not have significant impact on LCOE.

The availability of similar assessments allowed for a comparison of the selected results of our case study. In agreement with previous works, we determined that the power transmission capacity increased strongly with the wind supply share. Furthermore and despite a different model setup concerning the distribution of power plants and the consideration of storage, the endogenously calculated grid capacities were also similar. At theoretical VRE shares of 40% and 60% with a balanced mix of PV and wind, we noted 117 TWkm and 170 TWkm of transmission capacity across Europe, respectively, which is comparable to 150 TWkm at a theoretical VRE share of 50% identified in previous research [9]. In one scenario variation [12], reported a transmission grid extension of eight to nine times the existing grid in the parameter space that overlaps ours. The maximum grid capacity calculated by REMix for high VRE shares reached 320 TWkm, which is 10 times the approximation of the current high-voltage grid obtained by considering the 2010 transmission interconnector capacities and the node distances listed in Table 7. This slightly higher value can be explained by the predefinition of regional generation capacities in Ref. [12], which is likely to reduce power transmission.

Our case study underlines the importance of energy storage in supply systems with high VRE shares. According to the REMix results, storage converter capacities of up to 61% of the peak load are installed, and up to 20% of the annual demand is stored. A comparison to [12], in which storage is not considered, revealed that storage can significantly contribute to the avoidance of VRE curtailment. At balanced mixes with 60% and 100% VRE, we found curtailments equivalent to 3% and 20% of the demand, respectively, which is significantly less than the 10% and 30% obtained by Ref. [12]. A comparison of the backup capacity requirements calculated by REMix with findings of [12] revealed that our results are very similar at low VRE shares; owing to partial replacement of backup capacity by storage, they are lower by 20% at high VRE shares.

Lacking better information [12], and [9] set the share of offshore wind capacity to 50% of the total wind power capacity installation. However, we found that 32% was the highest value of the model-endogenous offshore share in the total wind capacity installation in any scenario and thus suggest consideration of this result as a more appropriate offshore share limit in future studies for Europe. For the considered technologies, model parameterisation, and scenarios, our results indicate the existence of economic upper limits in the supply share of both PV and wind, which were reached at about 60% and 70% of the overall generation, respectively. Beyond these levels, additional capacity mostly increased curtailment. Both values must not be regarded as technical maximum but instead represent cost minima at the given system setup. Owing to the negligence of storage capacity expansion [12], presented a lower value of about 50% for the maximum PV share.

According to the REMix results, the minimum system costs were incurred for VRE shares of about 60% in the wind-dominated and balanced supply mix. The results can be moved towards higher VRE shares either by the achievement of lower wind, PV, storage, or grid costs or by political measures that further increase the cost of fossil fuel use. Across all scenarios, the LCOE was between 0.088 €/kWh and 0.121 €/kWh, which is the same order of magnitude as the values calculated by Ref. [9].

The REMix results revealed that CSP is competitive at low VRE shares. With an increase in VRE share, it was gradually eliminated from the system and was found to be more expensive than gas power plants as soon as no backup capacity is needed with more than 4000 annual full-load hours. In contrast to CSP, biomass and geothermal power were not competitive in any scenario. This result suggests that their costs would have to be decreased more or that additional revenues, e.g. for negative emissions in biomass power plants with CCS or for heat delivered to district heating systems, would have to be generated to create economic power generation in these plants. In this account, the profitability of current biomass power plants arises from their operation in cogeneration mode, the availability of subsidies, or lower fuel costs than those considered here. Our sensitivity analysis showed that biomass becomes competitive if variable power generation costs can be reduced to a level of approximately 40 €/MWh.

According to our modelling results, long-term hydrogen storage was cost-effective only in one specific case with shares of about 65% wind and 15% PV supply. This implies that at any other supply mix, balancing is achieved at lower costs using other storage,

transmission, and conventional backup. At higher wind supply shares, the increasing usage of offshore turbines reduces the operation hours of dispatchable alternatives, making gas turbines more economic than long term storage. Considering the significantly lower investment costs, which might be realized by using salt caverns for storage, hydrogen storage is also used in scenarios with a wind supply share of 50% or more. Earlier REMix calculations showed that higher CO_2 emission costs can also have a favourable impact on the application of long-term storage [22].

7. Conclusion

This paper introduces the REMix energy system model by application to systematic scenario analysis, which illustrates its structure and functionalities. The results show least-cost configurations of the European power system at different VRE shares and solar-to-wind ratios. In the case study presented, REMix demonstrates its ability to reflect power demand, generation, transmission, and storage in an approximated manner.

Our results show that evaluations of least-cost power supply systems with high VRE shares must consider integrated capacity expansion of all backup generation technologies including CSP as well as storage and the power grid. This arises from their intrinsically different system functions with regard to their ability to balance short-, medium-, and long-term fluctuations of VRE power generation. In addition to the technologies assessed in this work, future research must account for further flexibility options, particularly enhanced coupling of the power, heating, and transport sectors through controlled battery charging of electric vehicles, flexible production of synthetic fuels, and electric heating and cogeneration/trigeneration combined with TES. In addition, future studies should improve the representation of the power grid by considering a finer spatial resolution.

In our case study and with the applied technology and cost parameters, balancing of VRE fluctuations is mostly provided by CSP, as well as coal and gas power plants with CCS at low VRE shares, and by battery storage and power transmission at high VRE shares. In contrast, biomass, geothermal, and nuclear power were not cost-effective, and hydrogen storage was cost-effective in only one scenario. In particular, the results clearly indicate that storage becomes important at high solar shares and power transmission is important at high wind shares. They are, however, subject to a high dependency on the applied cost assumptions. Furthermore, the system configuration might also change if regions with better solar resources are included in the assessment. Power import from CSP plants in North Africa and the Middle East might be an option for providing additional backup capacity for European power supplies and should be analysed in future research. In this account, the expansion of the assessment area towards Russia should also be considered.

Although our results regarding transmission line expansion at high VRE shares are highly similar to those of earlier assessments, we detect considerably lower curtailments, enabled by the use of CSP and additional storage systems. These findings can support generic modelling of VRE integration in energy system or integrated assessment models. In this regard, we recommend modelling CSP and storage explicitly so that system interactions can be reproduced such as those regarding backup capacity and curtailment.

We find that even at the highest VRE shares, between 1% and 8% of the demand is covered by conventional power plants even when curtailments of close to 30% of annual demand are present. This shows that even though sufficient energy from VRE could be made available, gas turbines and CCGT plants can still be competitive from the system perspective, however, with low capacity utilization at high VRE shares. If the current electricity market structure does not support the maintenance of such backup power stations in the future, our results provide an argument for long-term adjustments of electricity market regulation.

Independent of the applied VRE share, we find that supply costs are generally lower in wind-dominated scenarios. However, our results also indicate that the mix of PV and wind power has only a small impact on the overall cost. Therefore, the achievable supply costs at a given VRE share increase only to a minor extent if higher costs of either PV or wind are considered. Furthermore, this result implies that decisions on the future mix of PV and wind energy in Europe can be made on the basis of important factors other than supply cost such as security of supply, technology acceptance, availability of rare materials, and economic development. The sensitivity analysis indicates that variations in backup, storage, or grid costs have only a limited effect on the overall supply costs in Europe. This implies that the resulting power supply costs are rather robust against changes in the costs of single technologies.

Despite the small changes in system costs, the considered technology cost variations can, however, lead to significant differences in system structure and operation. This is particularly true for the case of higher CCS and lower biomass fuel costs at low VRE shares and that for lower or higher battery costs and higher power grid costs at high VRE shares. Furthermore, the sensitivity analysis shows that the choice of the historical weather year has a strong influence on the balancing demand in terms of both capacity and energy. This result highlights the need for more systematic evaluations of the interrelation between least-cost power supply structures and the choice of both VRE generation and demand profiles.

Owing to the uneven geographic distribution of solar and wind energy potentials, the predefined VRE supply structure has a significant impact on the regional allocation of power generation; solar-dominated systems are characterised by northwards, wind-dominated systems by southwards power flows. The analysis of regional results shows that in some scenarios and regions, the level of domestic generation can be as low as 20% and as high as 1000% of the corresponding demand. Despite the significantly higher grid capacity, a more regionally balanced distribution of power generation is available in the wind-dominated scenarios. The application of a minimum domestic generation capacity is expected to have a significant impact on the results. In any case, it would lead to higher costs because less attractive sites for VRE would have to be exploited.

Our results add to the assessment of balancing requirements associated with VRE integration in the wide parameter space. This, in addition to VRE shares and proportions, consists of assumptions on national or continental supply system development as well as power demand, costs, resources, and technological parameters. Its findings should be considered by policy makers who approve research and development funding and decide on future regulatory frameworks of power markets.

Acknowledgements

Dr. Wolfram Krewitt originally conceived the development of an energy system model focused on renewable energy technologies. After the first prototype of REMix was designed in a PhD thesis, further development of the model was funded mainly by the German Federal Ministry for Economic Affairs and Energy (BMWi) and by the German Federal Ministry for the Environment, Nature Conservation, Building and Nuclear Safety (BMU) within several research projects (grant numbers BMWI-FKZ 0328005A, BMWI-FKZ 0328009, BMWI-FKZ 03ET4020A, and BMU-FKZ 03MAP146). We are grateful to all colleagues of our department for numerous fruitful discussions on REMix's development and application.

Appendix

Table 4
Regional values of biomass and geothermal resources, VRE capacity limits, and hydro power capacities according to [14] and electricity demand according to [20]. ROTR refers to run-of-the-river hydro stations. Region definitions are listed in Table 3.

Region	Biom.	Geoth.	CSP	PV	Onsh.	Offsh.	Hydro	Reservoir Hydro		Pumped Hydro		Demand
	Resource		Max. Cap.				ROTR	Conv.	Stor.	Conv.	Stor.	
	TWh(ch)/a		GW(th)		GW		GW	GW	TWh	GW	GWh	TWh/a
Alps	54	32	0	372	22	0	16.4	15.5	12.1	6.2	43.4	121
BalkansNorth	66	168	0	547	89	31	11.77	0.4	0.4	0.03	0.2	152
BalkansSouth	38	111	42	950	67	122	8.0	3.1	3.5	0.8	5.9	114
Baltic	33	13	0	112	36	93	1.7	0	0	0.9	6.3	35
BeNeLux	34	34	0	561	9	97	0.2	0	0	1.3	9.1	199
CentralEast	155	176	0	693	81	50	4.4	1.0	1.1	1.4	10.0	258
CentralSouth	71	159	0	205	36	61	2.5	0	0.0	0	0	82
Denmark-W	30	12	0	70	6	103	0	0	0	0	0	22
East	132	154	0	401	213	120	4.9	0	0	0	0	285
France	452	359	19	1128	110	252	13.8	12.3	10.4	4.9	34.5	474
Germany	225	223	0	1373	55	72	4.2	0.4	0.4	5.9	41.5	514
Iberia	84	94	1566	2817	153	140	8.6	15.5	34.3	4.5	31.7	341
Italy	66	107	103	625	62	166	15.2	3.4	3.6	8.1	56.4	332
Nordel	208	4	0	1303	235	728	37.6	10.4	103.7	0.8	5.6	343
UK-IE	77	45	0	1470	50	1053	1.6	0.1	0.2	3.1	21.6	374

Table 5
Power generation technology parameters extracted or derived from Refs. [24,25].

Technology	η_{el} %	f_{avail} %	$c_{specInv}$ €/kW	c_{OMFix} % of invest/a	c_{OMVar} €/MWh	t_a a
Solar PV	n.a.	95.0%	720	1.0%	0	20
Wind onshore	n.a.	92.0%	900	4.0%	0	20
Wind offshore	n.a.	92.0%	1800	5.5%	0	20
730 (power block)						
CSP	37.0%	95.0%	192 (solar field)	2.5%	0	25
19 (thermal storage)						
Biomass	45.0%	90.0%	2000	4.0%	2	25
Geothermal	11.0%	95.0%	7600	4.5%	0	20
Run-of-the-river hydro	n.a.	95.0%	4000	5.0%	0	60
Reservoir hydro	90.0%	98.0%	4000	5.0%	0	60
Gas turbine (GT)	46.5%	94.8%	400	4.0%	0	25
GT-CCS	39.5%	94.8%	900	4.0%	7	25
CCGT	62.1%	96.0%	700	4.0%	0	25
CCGT-CCS	53.1%	96.0%	1200	4.0%	7	25
Coal	50.9%	89.6%	1500	4.0%	0	25
Coal-CCS	43.9%	89.6%	2000	4.0%	12	25
Nuclear	30.9%	90.0%	5000	4.0%	0	25

Table 6
Electricity storage technology parameters. Costs for converters conversion of PSH and hydrogen storage include pump/PEM electrolyzer electrolyser and turbine expenses

Technology	η_{charge} %	$\eta_{discharge}$ %	η_{self} %/h	f_{avail} %	$c_{specInv}$ €/kWh; €/kW	t_a a	c_{OMFix} % of invest/a
RFB	90%	90%	0%	98%	100 (Stor.); 300 (Conv.)	20	3%
PSH	89%	90%	0.001%	98%	640 (Conv.)	20	3%
Hydrogen	70%	57%	0%	95%	1 (Stor.); 900 (Conv.)	30; 15	3%

Table 7
Distances between considered model regions. Region definition are listed in Table 3.

Connection	Distance in km
Alps–CentralEast	646
Alps–CentralSouth	443
Alps–Italy	507
BalkansNorth–BalkansSouth	471
BalkansSouth–East	1161
BalkansSouth–Italy	965
Baltic–East	830
Baltic–Nordel	844
CentralEast–Baltic	720
CentralEast–CentralSouth	560
CentralEast–East	832
CentralEast–Nordel	1385

(*continued on next page*)

Table 7 (*continued*)

Connection	Distance in km
CentralSouth–BalkansNorth	414
CentralSouth–East	1016
CentralSouth–Italy	608
Denmark-W–Nordel	997
Denmark-W–UK-IE	894
East–BalkansNorth	790
France–Alps	741
France–BeNeLux	577
France–Iberia	885
France–Italy	863
Germany–Alps	441
Germany–Baltic	1127
Germany–BeNeLux	362
Germany–CentralEast	579
Germany–Denmark-W	561
Germany–France	764
Germany–Nordel	1496
Germany–UK-IE	1024
UK-IE–BeNeLux	682
UK-IE–France	946
UK-IE–Nordel	1694

References

[1] Herbst A, Toro F, Reitze F, Jochem E. Introduction to energy systems modelling. Swiss J Econ statistics 2012;148(2):111–35.

[2] Connolly D, Lund H, Mathiesen B, Leahy M. A review of computer tools for analysing the integration of renewable energy into various energy systems. Appl Energy 2010;87(4):1059–82.

[3] Després J, Hadjsaid N, Criqui P, Noirot I. Modelling the impacts of variable renewable sources on the power sector: reconsidering the typology of energy modelling tools. Energy 2015;80:486–95.

[4] Rasmussen Morten Grud, Andresen Gorm Bruun, Greiner Martin. Storage and balancing synergies in a fully or highly renewable pan-European power system. Energy Policy 2012;51:642–51.

[5] Rodriguez RA, Becker S, Andresen GB, Heide D, Greiner M. "Transmission needs across a fully renewable European power system. Renew Energy 2014;63:467–76.

[6] Heide Dominik, von Bremen Lueder, Greiner Martin, Hoffmann Clemens, Speckmann Markus, Bofinger Stefan. Seasonal optimal mix of wind and solar power in a future, highly renewable Europe. Renew Energy 2010;35(11):2483–9.

[7] Becker S, Rodriguez R, Andresen G, Schramm S, Greiner M. Transmission grid extensions during the build-up of a fully renewable pan-European electricity supply. Energy 2014;64:404–18.

[8] Denholm Paul, Hand Maureen. Grid flexibility and storage required to achieve very high penetration of variable renewable electricity. Energy Policy 2011;39(3):1817–30.

[9] Rodriguez Rolando A, Becker Sarah, Greiner Martin. Cost-optimal design of a simplified, highly renewable pan-European electricity system. Energy 2015;83:658–68.

[10] Jensen VT, Greiner M. Emergence of a phase transition for the required amount of storage in highly renewable electricity systems. Eur Phys J Special Top 2014;223(12):2475–81.

[11] Schaber Katrin, Steinke Florian, Hamacher Thomas. Transmission grid extensions for the integration of variable renewable energies in Europe: who benefits where? Energy Policy 2012;43:123–35.

[12] Schaber Katrin, Steinke Florian, Mühlich Pascal, Hamacher Thomas. Parametric study of variable renewable energy integration in Europe: advantages and costs of transmission grid extensions. Energy Policy 2012;42:498–508.

[13] Stetter Daniel. Enhancement of the REMix energy system model: global renewable energy potentials, optimized power plant siting and scenario validation. Universität Stuttgart; 2014. http://dx.doi.org/10.18419/opus-6855. PhD thesis.

[14] Scholz Y. Renewable energy based electricity supply at low costs: development of the REMix model and application for Europe. Universität Stuttgart; 2012. http://dx.doi.org/10.18419/opus-2015. PhD thesis.

[15] Kühnel Sven. Investigation of the variability of solar and wind electricity generation potantials in Europe and North Africa. Oldenburg: Karl von Ossietzky Universität; 2013. Master's thesis.

[16] Gils HC. Balancing of intermittent renewable power generation by demand response and thermal energy storage. Universität Stuttgart; 2015. http://dx.doi.org/10.18419/opus-6888. PhD thesis.

[17] Gils Hans Christian. Economic potential for future demand response in Germany - modeling approach and case study. Appl Energy 2016;162:401–15.

[18] Luca de Tena D. Large scale renewable power integration with electric vehicles. Universität Stuttgart; 2014. http://dx.doi.org/10.18419/opus-2339. PhD thesis.

[19] ENTSO-E, "ENTSO-E load and consumption data."

[20] Trieb F, Schillings C, Pregger T, O'Sullivan M. Solar electricity imports from the Middle East and North Africa to Europe. Energy Policy 2012;42:341–53.

[21] Scholz Yvonne, Christian Gils Hans, Pregger Thomas, Heide Dominik, Cebulla Felix, Cao Karl-Kiên, et al. Möglichkeiten und Grenzen des Lastausgleichs durch Energiespeicher, verschiebbare Lasten und stromgeführte KWK bei hohem Anteil fluktuierender erneuerbarer Stromerzeugung. 2014. http://elib.dlr.de/93240/.

[22] Scholz Y, Gils HC, Pietzcker R. Application of a high-detail energy system model to derive power sector characteristics at high wind and solar shares. Energy Econ 2016. p. in Press.

[23] Luca de Tena Diego, Pregger Thomas. Impact of electric vehicles on a future renewable energy based power system in Europe with the focus on Germany. Appl Energy 2017 [submitted for publication].

[24] Danish Energy Agency and Energinet.dk. Technology data for energy plants. May 2012.

[25] Pregger Thomas, Nitsch Joachim, Naegler Tobias. Long-term scenarios and strategies for the deployment of renewable energies in Germany. Energy Policy 2013;59:350–60.